Application Note

Direct Time of Flight LiDAR Design Using LMH13000 and LMH32401

ABSTRACT

Light detection and ranging (LiDAR) is a core ranging technology which uses laser light to measure distances. LiDAR can be used to create precise, three-dimensional (3D) maps and structural point clouds of objects and environments. LiDAR is mainly of two types: direct time of flight (dToF) and indirect time of flight (iToF). dTOF determines object distance by measuring the round-trip travel time of nanosecond-scale laser pulses and converting that timing into range, while iToF uses continuous modulated light to measure the phase shift (wave delay) between the emitted and returned signals. This design describes how LMH13000 and LMH32401 can be used to transmit and receive (respectively) nanosecond light pulse for measuring the distance using direct time of flight technique.

Table of Contents

Trademarks

All trademarks are the property of their respective owners.

1 Introduction

LiDAR is a remote-sensing technology that measures distance by emitting short laser pulses and timing how long the pulses take to return after reflecting off objects, a principle known as time-of-flight (ToF). By repeating this process millions of times per second and combining each distance measurement with precise angular or positional information, LiDAR systems can generate high-resolution 3D point clouds that accurately represent real-world environments.

Within LiDAR, iToF and dToF represent two different ways of extracting distance. These two are fundamentally different LiDAR depth-sensing techniques that both rely on measuring how long light takes to travel to a target and back, but extract that timing information in very different ways.

In iToF, the transmitter emits amplitude-modulated or phase-modulated continuous light, and the receiver measures the phase shift between the emitted and received echo signals. Because speed of light is fixed, the phase shift directly translates to the distance traveled by the light in the round trip. In contrast, dToF sends short laser pulses and uses fast detectors and timing circuits to measure the exact arrival time of each echo pulse with picosecond precision, enabling long range, high accuracy distance measurement.

This article explains how Texas Instruments' laser driver LMH13000 and integrated transimpedance amplifier LMH32401 can be used to design the front end for dToF LiDAR.

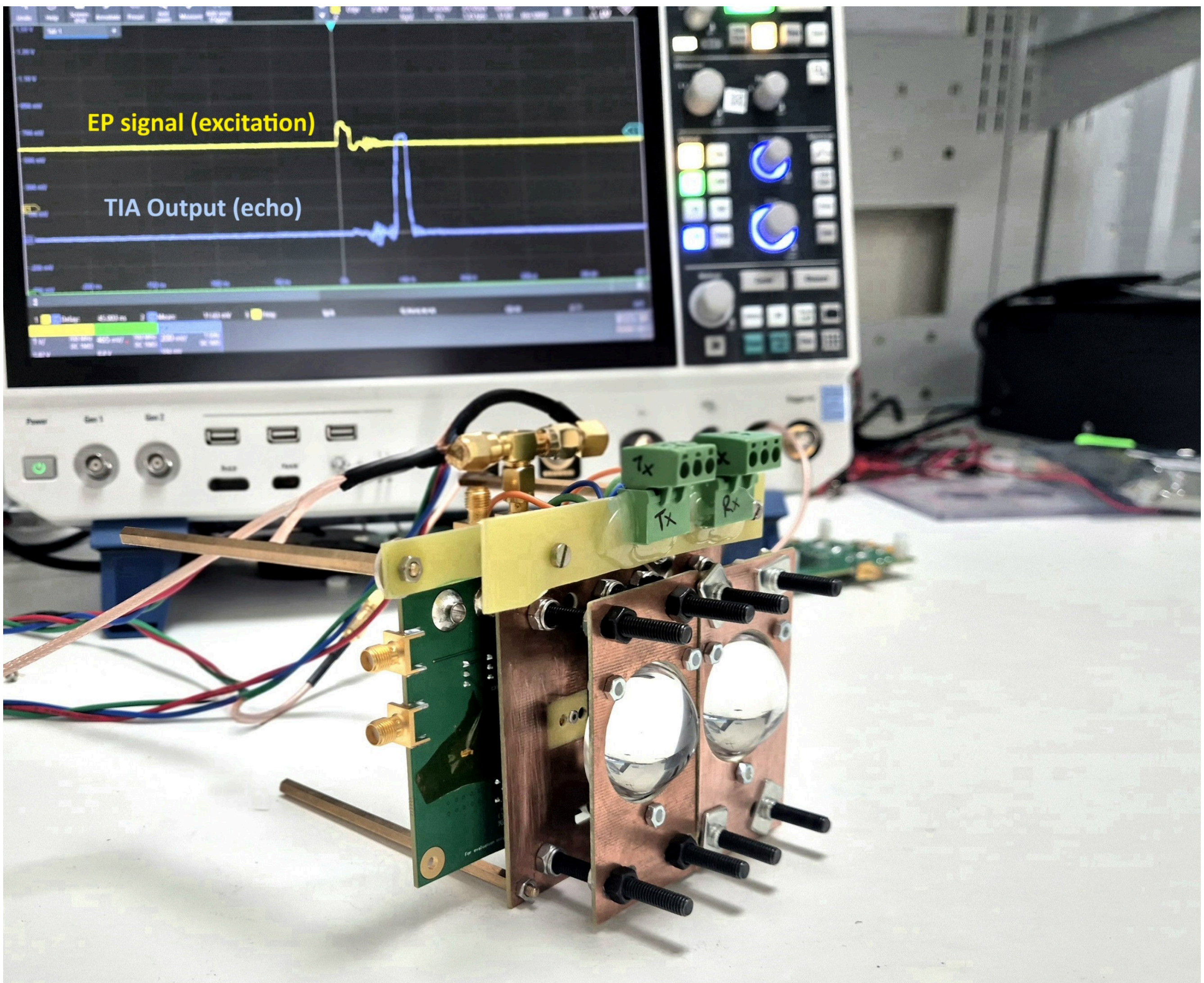

Figure 1-1. LiDAR Setup

2 Description

As explained, the direct time of flight is a technique that measures the time (Δt) light takes to travel from source to an object and back. From this information, the distance of the object from the source can be determined. To implement this in hardware, we need a transmitter or source which can generate narrow high power light pulse, and a receiver sensitive enough to detect the weak echo optical pulse signal reflected after hitting the object. Both transmitter and receiver are typically placed next to each other facing the object whose distance has to be measured. This makes sure that the transmit path signal and the reflected path signal have the same distance to travel. In this way, the distance (d) of the object from the source is given by speed of light (c), multiplied by half the total time of flight (Δt) of the light pulse.

$$d = c \times \frac{\Delta t}{2} \quad (1)$$

For this design, a laser (TL90AT03) is used as a light source, which is driven by TI's laser driver, LMH13000. The LMH13000 pulses the laser to emit a short burst of infrared light. The optical output light from the laser is collimated using a lens and is then transmitted, which then travels through open space and gets reflected once the light hits any object in the path.

The reflected light is collected by a converging lens and focused onto an avalanche photodiode (APD), which converts the optical pulse into a small current. This current is then amplified and converted to a voltage signal using a transimpedance amplifier LMH32401, producing a clean electrical signal that represents the arrival of reflected pulse.

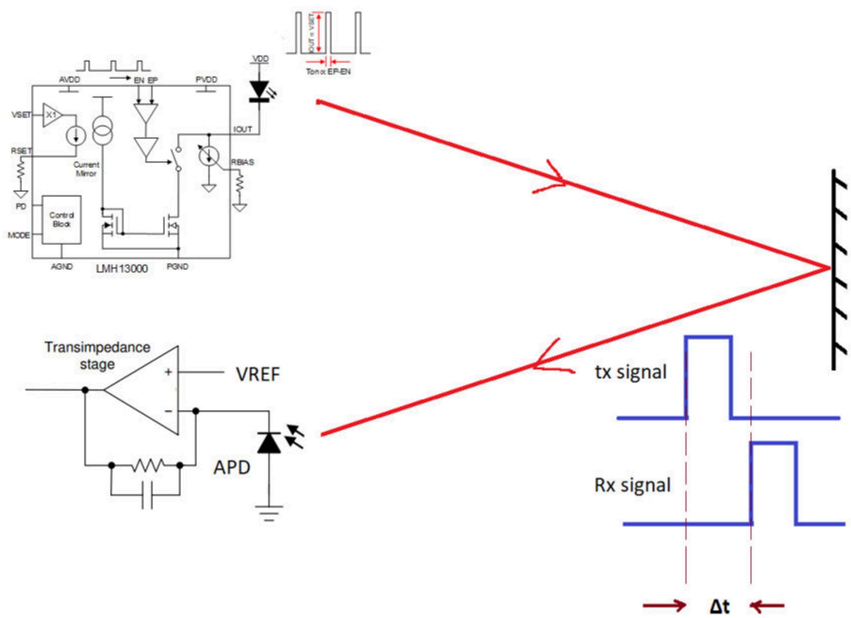

Figure 2-1. LiDAR Setup

3 Transmitter

The transmitter subsystem integrates a high-power optical emitter with a precision current-drive stage to generate narrow, high-energy optical pulses required for long-range LiDAR operation. The optical source selected for this design is Osram's TL90AT03 laser diode, a 905nm infrared device capable of sustaining pulsed currents up to 20A, making the diode an excellent choice for long range time-of-flight applications. To drive this laser, the design employs Texas Instruments' LMH13000, a voltage-controlled current source optimized for fast, accurate laser pulsing. The LMH13000 delivers sub-nanosecond rise and fall times without requiring an external FET, significantly simplifying the transmitter architecture while maintaining excellent pulse fidelity. Laser peak current is programmed through the VSET pin, which provides a linear relationship between the applied voltage and the resulting output current. Pulse timing and repetition are controlled through the EP/EN input, enabling precise modulation of the emitted optical pulse. The device supports two selectable operating modes — Mode 0 (5mA to 1A) and Mode 1 (50mA to 5A) — allowing designers to configure the driver for different power levels or operating conditions. Because the LMH13000 is inherently a current-output device, multiple drivers can be paralleled to scale the available peak current beyond 5A, enabling flexible transmitter configurations that meet the requirements of high-range, high-resolution LiDAR systems.

3.1 Optical Power Versus Measuring Distance

In LiDAR systems, optical output power and distance measurement are fundamentally linked together. Simply put, distance determines how much power returns to the sensor, while output power dictates the maximum distance the LiDAR can measure.

3.2 The Inverse-Square Law and Distance

As a laser light pulse travels through the air, the light spreads out. When the laser pulse hits a target, that target scatters the light in all directions. The portion of light that reflects back to the LiDAR's receiver is governed by the inverse-square law.

The power of the returning light drops sharply as distance increases. If you double the distance to an object, the returning optical power drops by a factor of four ($1 \div 2^2$). At twice the distance, the received signal is only 25% as strong.

Simply put, distance determines how much power returns to the sensor, while output power dictates the *maximum distance* the LiDAR can measure.

3.3 Optical Power Determines Maximum Range

Because the return signal weakens so quickly over distance, a LiDAR system needs enough initial optical output power to make sure the returning light is stronger than the background noise (for example, sunlight).

High Peak Power: Emitting a highly powerful, short burst of laser light allows the system to detect distant objects because enough light survives the round-trip journey.

Safety Limits: Output power cannot be increased infinitely. Systems must often adhere to strict eye-safety regulations (Class 1 limits), which cap the maximum optical power depending on the laser's wavelength (commonly 905nm or 1550nm).

To achieve high distance measurement range, our target is to send a very high peak optical pulse power but for a very short duration such as 2ns to 3ns, while keeping the duty cycle in very small fraction -0.1% or below based on peak power. This makes sure that we get sufficiently strong echo optical pulse signal which our receiver can detect while still keeping the total optical power within the safe eye limit of a class 1 laser.

Figure 3-1 shows how LMH13000 can be used to drive a laser for transmitting the optical pulse for dTOF Lidar.

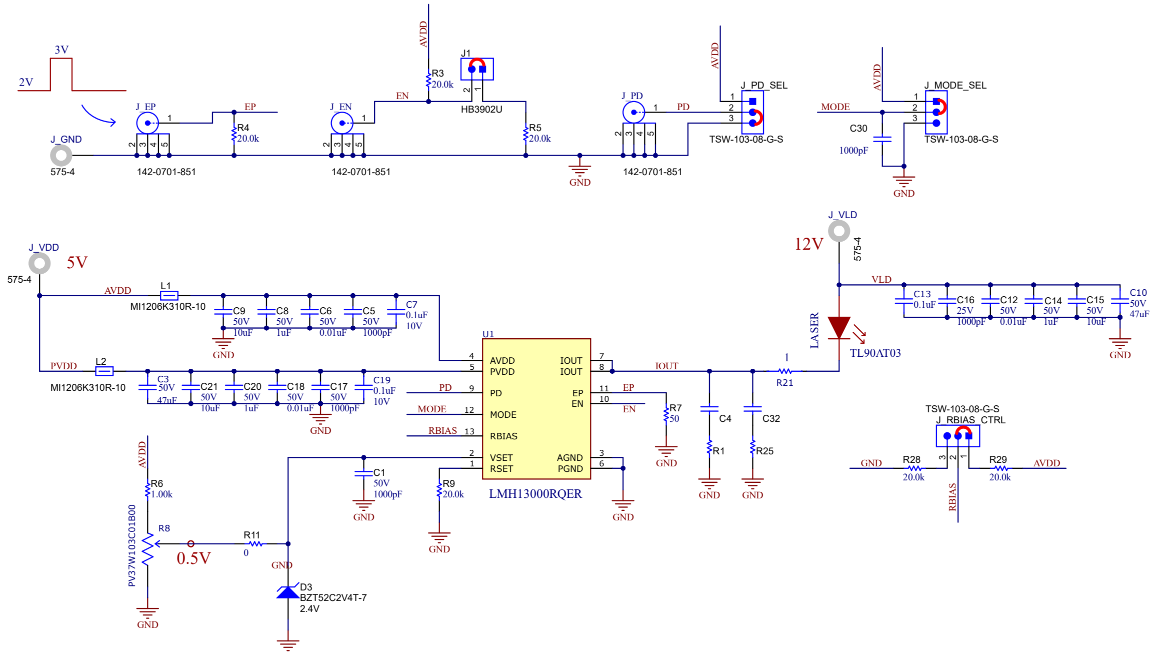

Figure 3-1. Transmitter Schematic

4 Receiver

The receiver subsystem converts the weak, time-delayed optical echo into a clean electrical signal that is an excellent choice for precise time-of-flight processing. The receiver subsystem consists primarily of an avalanche photodiode (APD) and a transimpedance amplifier (TIA). The APD serves as the optical front end, generating a proportional current in response to incident photons and providing internal gain through avalanche multiplication, which improves sensitivity for long-range LiDAR detection. This current is then converted into a usable voltage by the TIA, an operational amplifier configured with a feedback resistor (R_f) that establishes the transimpedance gain according to Equation 2:

$$V_{out} = I_{in} \times R_f \tag{2}$$

Because the op-amp maintains a virtual ground at the inverting input, the APD sees a stable bias point, maintaining linear and predictable current-to-voltage conversion. When additional gain is required, a secondary voltage-amplification stage can be added after the TIA.

Designing a high-performance receiver requires careful attention to stability, noise, and bandwidth. The APD and PCB traces introduce input capacitance that interacts with the feedback resistor to form a pole that can degrade phase margin and cause ringing or oscillation. To maintain stability, a small feedback capacitor, Cf, is placed in parallel with Rf, shaping the frequency response and maintaining well-damped transient behavior.

Input-bias current from the amplifier also contributes directly to DC error because the bias current gets multiplied by R_f; therefore, JFET-input or CMOS-input amplifiers with extremely low bias currents are preferred for minimizing offset.

Finally, gain and bandwidth are inherently linked: increasing R_f improves sensitivity but reduces bandwidth due to the combined effect of input capacitance and feedback impedance. Selecting the appropriate combination of APD, TIA architecture, and compensation components is essential for achieving the required dynamic range, noise performance, and timing accuracy in LiDAR receiver design.

4.1 Stability Consideration of TIA

If the photodiode is assumed to be an ideal current source, the output voltage of TIA is given by Equation 3:

$$V_{OUT} = \frac{-I_{PD} \times R_F}{(1 + j2\pi f R_F C_F)} \tag{3}$$

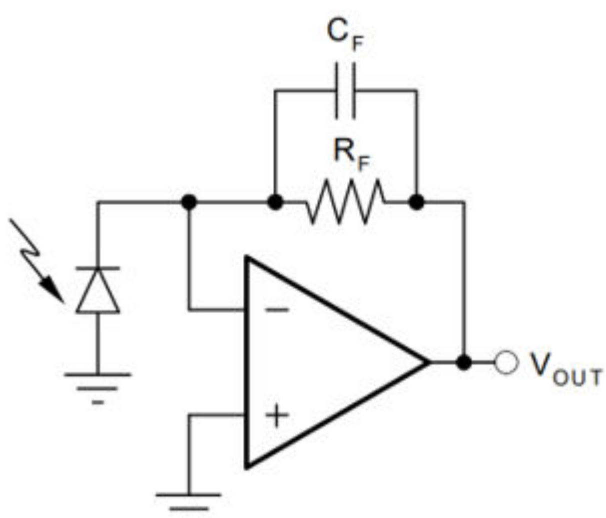

Figure 4-1. Ideal Photodiode TIA Circuit

For a practical implementation, the photodiode cannot be treated merely as an ideal current source. Instead, the device is more accurately modeled as an ideal current source in parallel with an equivalent shunt resistance, R_D, and junction capacitance, C_D. The op amp input capacitance also cannot be considered insignificant and must be included as part of C_D.

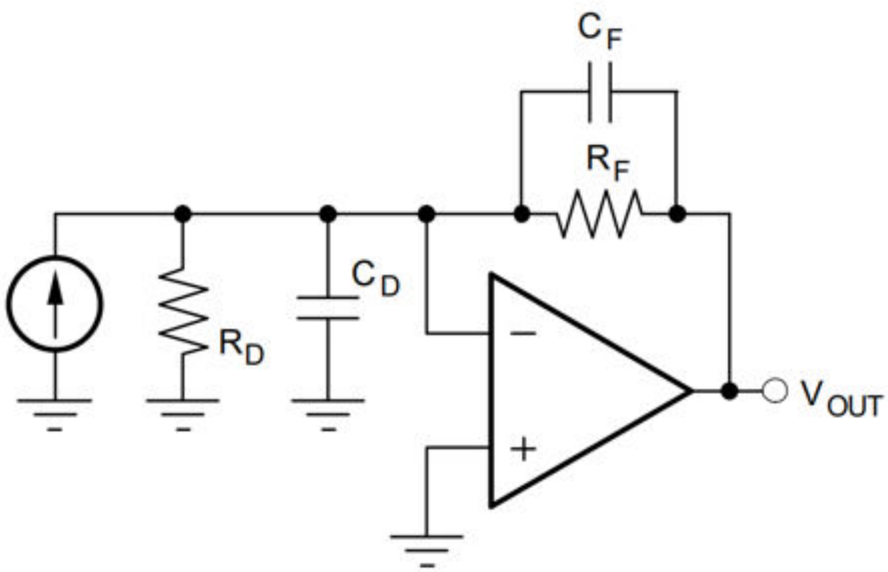

Figure 4-2. Photodiode Electrical Model with TIA

$$A_{CL}\left(f\right) = \frac{R_F + R_D}{R_D} \times \frac{1 + \frac{j2\pi f(R_F R_D)}{(R_F + R_D)}\left(C_F + C_D\right)}{(1 + j2\pi f(R_F C_F))} \tag{4}$$

$$A_{CL}\left(f\right) = \frac{R_F + R_D}{R_D} \times \frac{\left(1 + j\frac{f}{f_Z}\right)}{\left(1 + j\frac{f}{f_P}\right)} \tag{5}$$

$$\text{Here,} \quad f_P = \frac{1}{(2\pi R_F C_F)} \tag{6}$$

$$f_Z = \frac{1}{2\pi(R_F || R_D)(C_F + C_D)} \tag{7}$$

Generally, $R_D >> R_F$, $R_F||R_D = R_F$ and the DC gain also becomes unity.

$$f_Z = \frac{1}{2\pi R_F(C_F + C_D)} \tag{8}$$

This implies f_Z is always lower than f_P.

For the system to be stable, the f_P must lie inside the open loop curve of op amp.

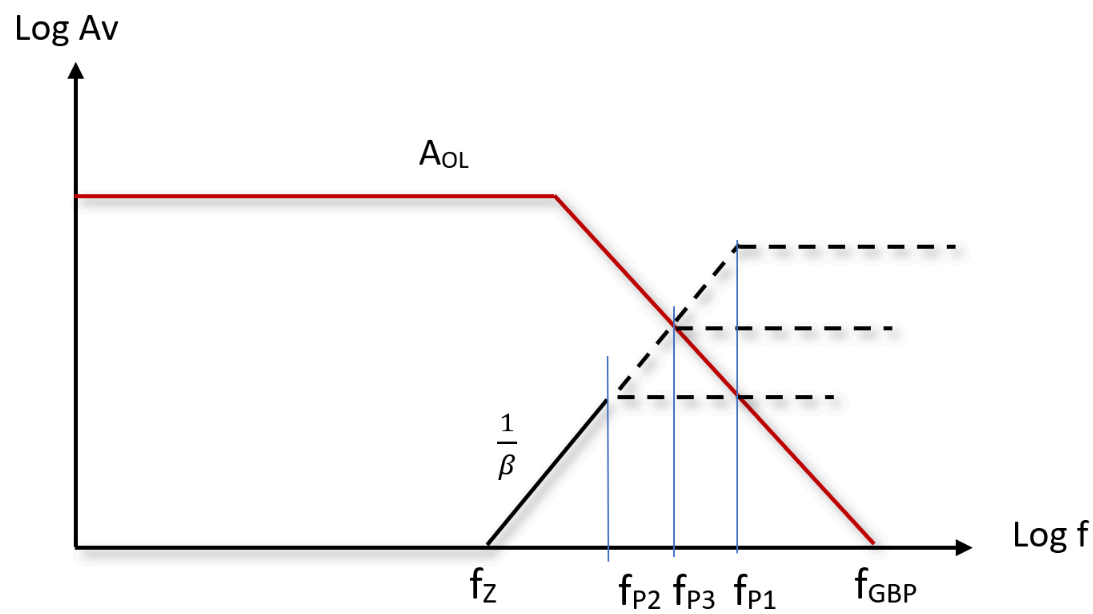

Figure 4-3. Open-Loop and Closed-Loop Response of TIA vs Frequency

Figure 4-3 shows three different scenarios for the intersection of the closed-loop response (inverse of the feedback factor) with the open loop gain curve. Instability occurs when the rate of closure of the two curves is 40dB. This happens when the f_P falls outside the open loop curve as in case of f_{P1} and the circuit, in this case, oscillates. If f_P lies inside the open loop curve like in the case of f_{P2}, the transimpedance circuit is unconditionally stable, but the stability in this case is traded off for transimpedance bandwidth. The best practice is to place the f_P on the open-loop gain curve as shown for f_{P3}.

Since f_P is determined by the feedback network, judicious selection of C_F. is all that is necessary. This process can be greatly simplified by noting that the high frequency asymptote for the noise gain is determined by capacitance values alone.

$$\text{For}\left(f > > f_P\right), \text{ACL} = \frac{C_F + C_D}{C_F} \tag{9}$$

For f_P to be on AOL curve,

$$\frac{\text{GBP}}{f_P} = \frac{C_F + C_D}{C_F} \tag{10}$$

On solving for C_F:

$$C_F = \frac{1}{(4\pi R_F \text{GBP})} \times \left(1 + \sqrt{1 + 8\pi R_F C_D \text{GBP}}\right) \tag{11}$$

Once the photodiode capacitance and op amp GBP are determined, the capacitance value of the feedback capacitor must be selected appropriate as per Equation 9 to Equation 11 to maintain stability.

$$f_P = \sqrt{\frac{\text{GBP}}{2\pi R_F C_D}} \tag{12}$$

This result indicates that, for a given op amp and photodiode, transimpedance bandwidth is inversely related to the square root of the feedback resistor. Thus, if bandwidth is a critical requirement, the best approach can be to opt for a moderate transimpedance gain stage followed by a broadband voltage gain stage.

4.2 Transimpedance Amplifier Selection: LMH32401

The LMH32401 is an integrated device which features a programmable gain transimpedance amplifier (TIA) stage followed by a fixed-gain, single-ended input to differential output amplifier stage and is designed mainly for LIDAR and pulsed ToF systems

The LMH32401 supports both photodiode sinking (fast recovery clamp) and sourcing (soft clamp with longer recovery) configurations. The device features a programmable-gain TIA stage followed by a fixed-gain differential output stage. For a particular photodiode capacitance, ;ow-gain configuration offers higher bandwidth, while high-gain provides lower input-referred noise (increasing output by ×X while noise increases only by √X). Gain is controlled through the GAIN pin: low for low-gain, high for high-gain mode

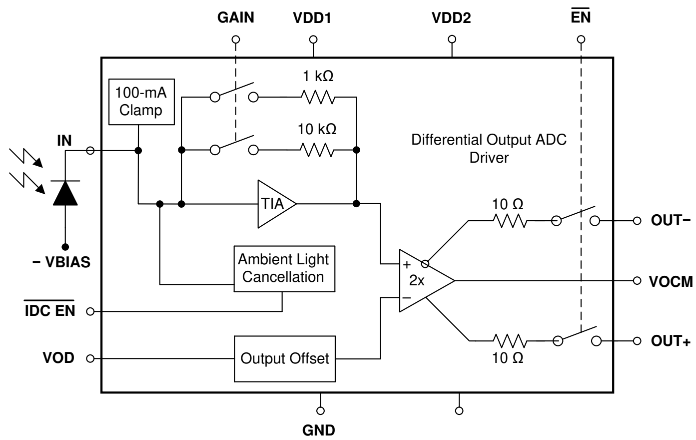

Figure 4-4. LMH32401 Block Diagram

The benefit of using LMH32401 is that the device does not require external compensation capacitor for wide range of input capacitor values. And based on the capacitance value of the photodiode, and the bandwidth requirement, users can select which gain-mode to use. Figure 4-5 and Figure 4-6 show the LMH32401 bandwidth at different input capacitor values for low gain and high gain mode respectively .

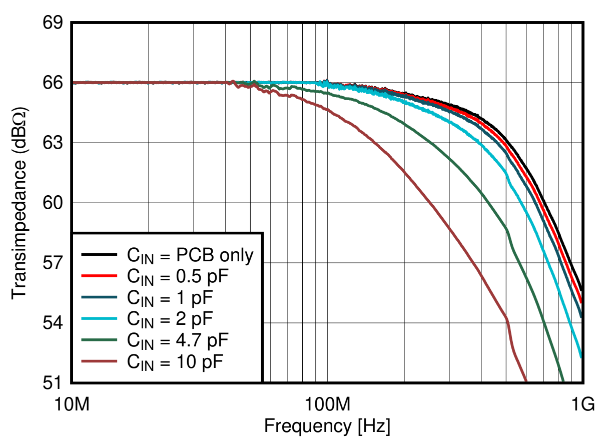

Figure 4-5. Small Signal Response vs Input Capacitance (Gain = 2K)

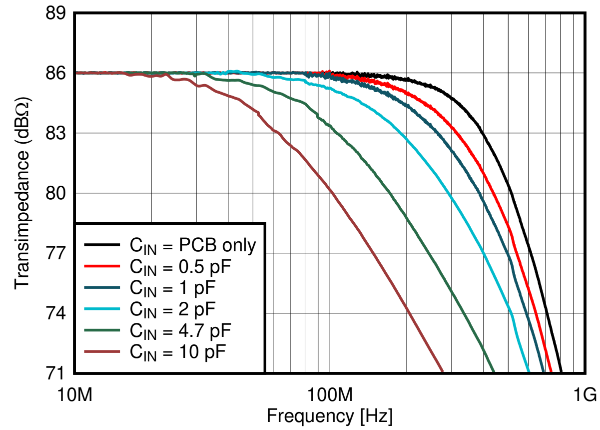

Figure 4-6. Small Signal Response vs Input Capacitance (Gain = 20K)

If additional gain is needed, a second amplifier can also be added as a next stage.

For this design, we have selected Marktech photodiode MTAPD-06-009 and biased the photodiode at -120V to achieve the APD gain of 100. At this bias voltage, the diode capacitance is approximately 1pF. The TIA LMH32401 is set at a gain of 20K, and from the graph above, the expected bandwidth is approximately 280MHz.

Because rise time = 0.35/BW for first order system, we can expect a rise time of approximately 1.25ns with this configuration.

Figure 4-7 shows the full schematic of the receiver.

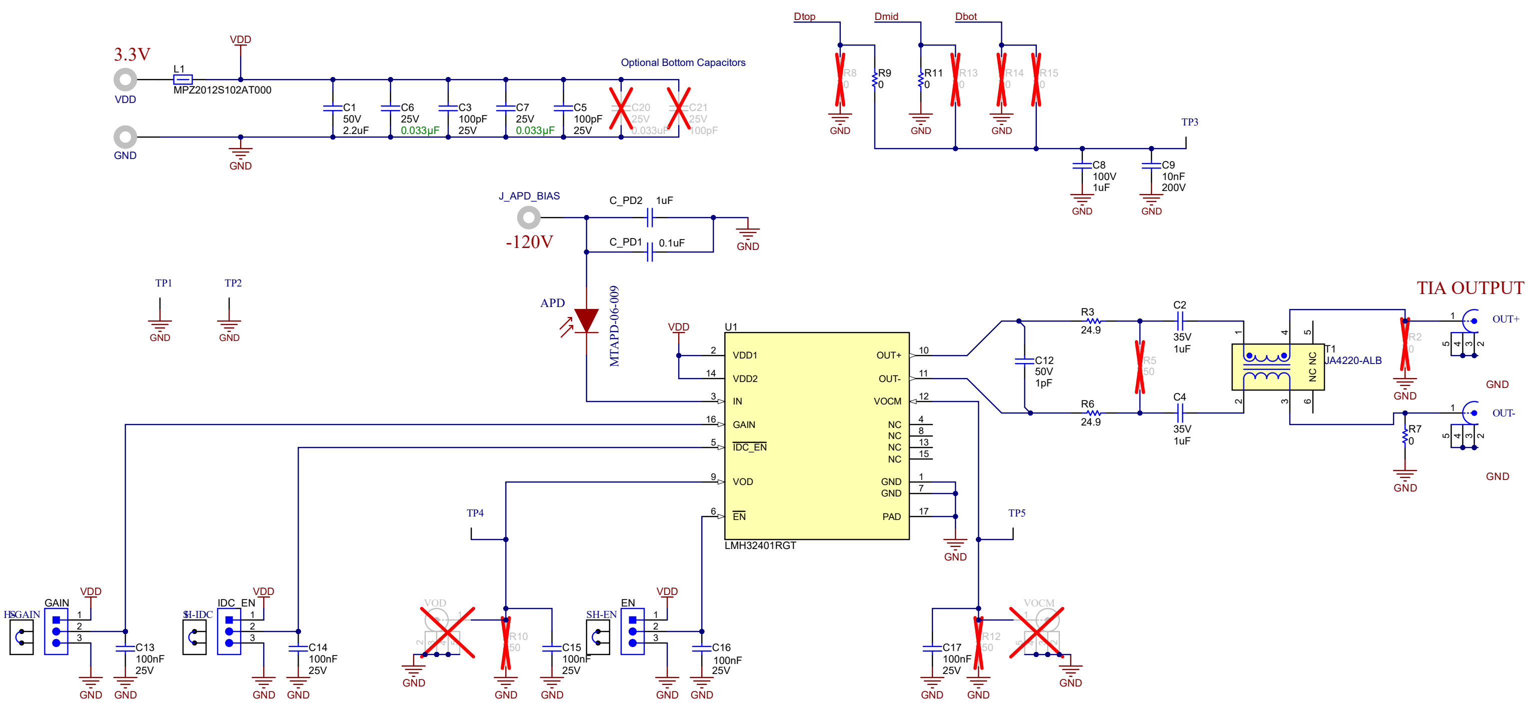

Figure 4-7. Receiver Schematic

5 Optical Housing Design

Most LiDAR systems use edge-emitting or VSCEL semiconductor laser diodes. Due to the physics of light diffraction through extremely small output apertures, the beam diverges rapidly and unevenly after exiting the semiconductor surface.

In edge emitting laser diodes, there are two main types of beam divergence along two orthogonal axes of the laser's PN junction: parallel and perpendicular. Due to the asymmetric geometry of an edge-emitting laser diode, the emission aperture parallel to the p-n junction is significantly wider than the aperture along the perpendicular axis, resulting in a wider initial beam waist along the parallel axis. Consequently, in accordance with the laws of optical diffraction, a narrower aperture induces a greater spatial spread. The perpendicular axis therefore exhibits a substantially higher divergence angle despite having a narrower initial beam waist. Because of this structural asymmetry, the raw beam exiting the laser diode rapidly deforms into an elongated elliptical shape rather than a symmetric circular profile. External collimating optics are therefore required to transform this strongly divergent, spreading beam into a well-collimated, parallel beam of light.

The laser diode, TL90AT03 used in this design which serves as the optical source of the transmitter (Tx), exhibits a parallel beam divergence of 10° and a perpendicular divergence of 25°. Collimation of the transmitted beam from this laser is achieved using a plano-convex lens with a 22mm focal length and a 35mm diameter.

An identical lens configuration is used on the receive (Rx) side of the optical path to converge and focus the returning echo optical pulse onto the active area of the avalanche photodiode (APD) sensor, as shown in Figure 5-1.

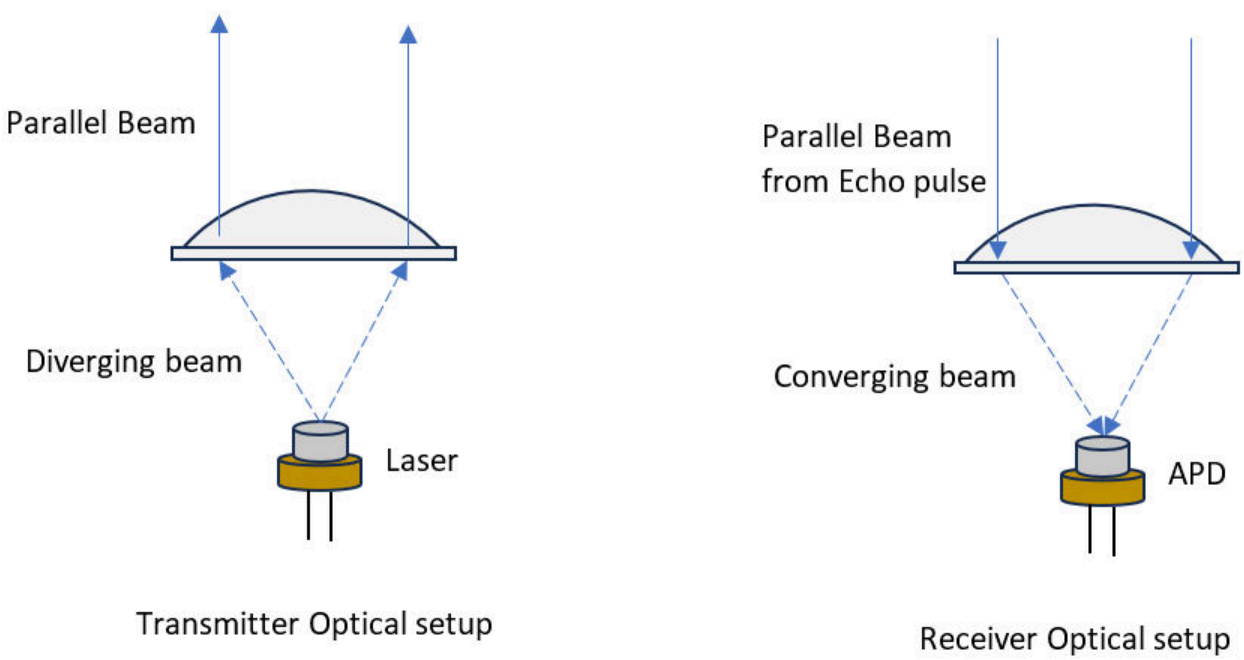

Figure 5-1. Optical Lens Setup for Tx and Rx

6 Measurement Setup

The ToF measurement relies on accurately determining the interval between the transmitted laser pulse and the received echo. In systems where the excitation signal driving the LMH13000 is used as the start reference, the propagation delay from the LVDS input of the driver to the current output must be carefully calibrated. This delay and the delay variation across temperature and process directly contributes to distance-measurement error if left uncompensated. A robust alternative is to derive the start reference by directly sensing the laser current, thereby eliminating dependence on the internal propagation characteristics of the driver. This is implemented by inserting a series sense resistor with the laser diode, which simultaneously serves as a damping element to improve transient behavior. The voltage developed across this resistor is level-shifted and conditioned using resistor and capacitor network, as shown in Figure 6-1, to generate a precise start-pulse reference that reflects the actual onset of optical emission.

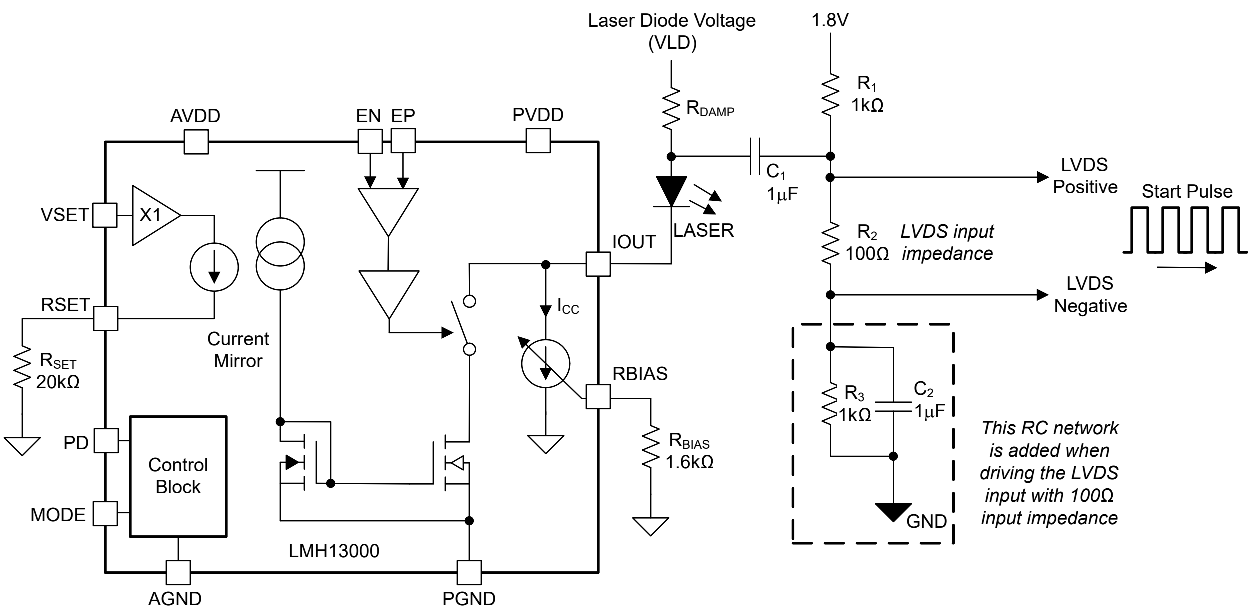

Figure 6-1. Start Reference Pulse Generation From IOUT Laser Current

For the experimental setup described in this application note, a delta-measurement approach is used rather than absolute distance measurement. Instead of determining the absolute distance of the object from the source, the system measures changes in distance relative to a baseline. This method inherently cancels fixed system delays from both the transmitter and receiver paths, including propagation delays within the LMH13000 and downstream signal-conditioning circuitry. As a result, the system achieves accurate relative-distance tracking without requiring explicit calibration of driver propagation delay or temperature-dependent timing variations.

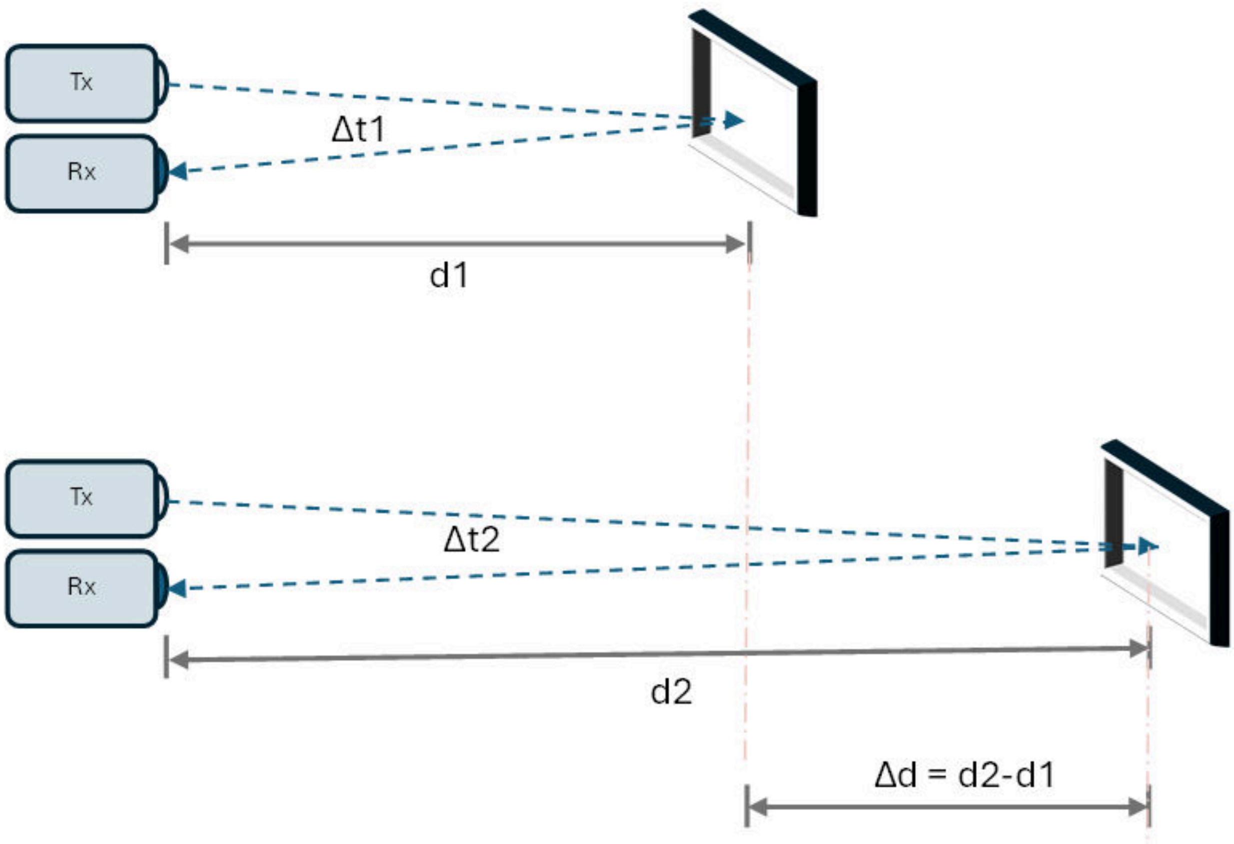

Figure 6-2. Block Diagram for Delta Distance Measurement Approach

$$\Delta t1 = \mathrm{tPD(Tx)} + \mathrm{tPD(Rx)} + \mathrm{ToF(d1)} \tag{13}$$

$$\Delta t2 = \mathrm{tPD(Tx)} + \mathrm{tPD(Rx)} + \mathrm{ToF(d1)} \tag{14}$$

$$\Delta t2 - \Delta t1 = \mathrm{ToF(d2)} - \mathrm{ToF(d1)} \tag{15}$$

$$= \mathrm{ToF}(\Delta d) \tag{16}$$

$$\Delta d = [\mathrm{ToF}(\Delta d) \times c]/2 = [(\Delta t2 - \Delta t1) \times c]/2 \tag{17}$$

where

- c = speed of light
- tPD(Tx) = the propagation delay of Tx circuit
- tPD(Rx) = the propagation delay of Rx circuit

7 Lab Measurement

The experimental setup is used to validate the accuracy of the direct time-of-flight measurement using the combined LMH13000 transmitter and LMH32401 receiver signal chain. The object is first placed at an initial position (d1), and the corresponding time-of-flight is captured on the oscilloscope by measuring the delay between the LMH13000 excitation signal (EP) and the processed echo signal from the LMH32401. The object is then moved 1.5m farther to a new position (d2), and the measurement is repeated again under identical operating conditions. The oscilloscope traces shown in Figure 7-1 and Figure 7-2 clearly indicate an increase in pulse delay that corresponds precisely to the known 1.5m displacement. Because the system measures relative time-of-flight, all fixed delays, such as driver propagation delay, APD and TIA processing latency, and signal-conditioning delays, cancel out, leaving only the true change in optical path length. These results confirm that the dToF architecture accurately resolves small distance changes and that the LMH13000 and LMH32401 combination provides a clean, reliable timing chain designed for high-precision LiDAR applications.

The scope shots shown in Figure 7-1 and Figure 7-2 measured time-of-flight waveforms showing the delay between the LMH13000 excitation pulse and the LMH32401 processed echo signal for object positions (d1) and (d2 = d1 + 1.5m). The observed increase in delay matches the expected change in optical path length.

Figure 7-1. ToF for d1 Distance

Figure 7-2. ToF for d2 Distance

$$\Delta d(\text{calculated from ToF}) = \frac{[(\Delta t2 - \Delta t1) \times c]}{2} = \frac{\left[(28.9 - 18.8)\text{ns} \times \left(2.997 \times 10^{8}\text{m/s}\right)\right]}{2} \cong 1.5\text{m} \tag{18}$$

8 Summary

The combination of TI's LMH13000 laser driver and LMH32401 TIA enables a highly accurate and easy to use dToF LiDAR architecture. The LMH13000 enables precious laser current control and delivers sub-nanosecond current pulses without external FETs, providing clean optical excitation for precise timing. Direct laser-current sensing to generate the start pulse further improves the accuracy and eliminates the need of propagation-delay calibration. On the receiver side, the LMH32401 provides low-noise, high-bandwidth transimpedance conversion designed for APD-based echo detection. The integrated gain control and stability features of the LMH32401 simplify compensation and layout, improving robustness across operating conditions. Together, these devices form a tightly coupled transmit-receive chain designed for high-resolution LiDAR. Lab measurements presented in the last section in this application note validate the performance, confirming excellent timing precision and signal integrity. Overall, LMH13000 and LMH32401 enable a compact, accurate, and production-ready dToF LiDAR design.

9 References

IMPORTANT NOTICE AND DISCLAIMER

TI PROVIDES TECHNICAL AND RELIABILITY DATA (INCLUDING DATASHEETS), DESIGN RESOURCES (INCLUDING REFERENCE DESIGNS), APPLICATION OR OTHER DESIGN ADVICE, WEB TOOLS, SAFETY INFORMATION, AND OTHER RESOURCES “AS IS” AND WITH ALL FAULTS, AND DISCLAIMS ALL WARRANTIES, EXPRESS AND IMPLIED, INCLUDING WITHOUT LIMITATION ANY IMPLIED WARRANTIES OF MERCHANTABILITY, FITNESS FOR A PARTICULAR PURPOSE OR NON-INFRINGEMENT OF THIRD PARTY INTELLECTUAL PROPERTY RIGHTS.

These resources are intended for skilled developers designing with TI products. You are solely responsible for (1) selecting the appropriate TI products for your application, (2) designing, validating and testing your application, and (3) ensuring your application meets applicable standards, and any other safety, security, regulatory or other requirements.

These resources are subject to change without notice. TI grants you permission to use these resources only for development of an application that uses the TI products described in the resource. Other reproduction and display of these resources is prohibited. No license is granted to any other TI intellectual property right or to any third party intellectual property right. TI disclaims responsibility for, and you fully indemnify TI and its representatives against any claims, damages, costs, losses, and liabilities arising out of your use of these resources.

TI’s products are provided subject to TI’s Terms of Sale, TI’s General Quality Guidelines, or other applicable terms available either on ti.com or provided in conjunction with such TI products. TI’s provision of these resources does not expand or otherwise alter TI’s applicable warranties or warranty disclaimers for TI products. Unless TI explicitly designates a product as custom or customer-specified, TI products are standard, catalog, general purpose devices.

TI objects to and rejects any additional or different terms you may propose.